National Conference

On

Sensor Technology

September 26-27, 2002

Convenor:
A.K. Kapoor

Secretary:
D.B. Singh

Organised by

Centre for Environment and Explosive Safety,
Defence Research Development Organisation (DRDO),
Ministry of Defence
at
CEES, Metcalfe House
Delhi - 110 054

Interacting Multiple Model Approach for Target Tracking and Trajectory Estimation

Jatinder Singh, Sudesh K. Kashyap, Girija G. and J. R. Raol
Scientists, Multi-Sensor Data Fusion Lab., Flight Mechanics and Control Division.
National Aerospace Laboratories, P.B. No. 1779, Vimanpura Post, Bangalore-560017
e-mail: jrraol@yahoo.com

Abstract: The Interacting Multiple Model (IMM) is a sub-optimal hybrid approach for effective target tracking and trajectory estimation. The main feature of the algorithm is its ability to switch from one model to another which makes it a potent tool to track maneuvering targets. A 2-model IMM approach is used as an example to describe the principles. 'assumptions and the procedures involved Its applicability to track maneuvering targets is demonstrated with simulated data. Comparison of results with those obtained from standard Kalman filter are given. The program is writien in MATLAB.

1 Introduction

Reliable tracking performance of maneuvering targets is of considerable interest today. Needles to say, some sort of adaptive state estimation is required to track a target whose behavior pattern keeps changing with time. The Interacting Multiple Model (IMM) is one such adaptive estimator which is based on the assumption that a finite number of models are required to characterize the target motion at all times. An optimal multiple model scheme/algorithm will be highly complex and computationally draining. IMM approach is a sub-optimal hybrid estimator. It is called hybrid since it is characterized by both continuous valued parameters Like target position, velocity and accelerations defined by the difference or differential form of state equations, as well as by the discrete stochastic process that controls the selection of a model corresponding to each behaviour mode. The IMM approach thus, performs both target state estimation as well as model selection from a given set of models. A finite state Markov chain with known transition probabilities is used to switch from one model to another. The mode transition probabilities, which constitute the transition matrix, are the design parameters for the algorithm. Initial mode probabilities are generally selected on the basis that a target is more likely to be in non-maneuver mode than in maneuver mode. The IMM algorithm consists of a set of model matched filter modules that interact in a certain way to yield the mode-conditioned state estimates. The modules can be Kalman Filters (KF) or Extended Kalman Filters (EKF) to account for the maneuvering target motion [1]. The tracking performance of both IMM and Kalman Filter (KF) algorithms is evaluated on simulated data of a maneuvering target. Sensitivity of IMM to its design parameters is also investigated. The study made in MATLAB shows that IMM gives better overall performance than KF and is very suitable for tracking maneuvering targets.

2 IMM Algorithm

IMM algorithm is a recursive estimator and consists of four major steps – interaction, mode-conditioned filtering. probability evaluation and combined state and covariance estimation. The case studies presented in this paper use KF modules in a 2-model IMM approach.

The base state model for a linear fixed-structure hybrid system can be described as follows

$$\begin{aligned} X(k+1) &= F_j(k)X(k) + G_j(k)w_j(k) && \forall\ j \in M \\ Z(k) &= H_j(k)x(k) + v_j(k) && \forall\ j \in M \\ & && j = 1,\ldots r \end{aligned} \tag{1}$$

where M is a set of possible r models (modes) and G_j denotes the process noise gain matrix. The process and measurement noises are Gaussian. mutually uncorrelated with zero mean and known covariances. It is clear from Eq. (1) that the system transition matrix F and the noise statistics can differ from mode to mode. The model switching is carried out using a Markov process with known transition probabilities. A first order homogeneous Markov chain for mode switching can be represented as

$$P\{M_j(k+1) \mid M_i(k)\} = p_{ij} \qquad \forall\ i,j \in M \tag{2}$$

This implies that. if M_i is the model in effect at k^{th} instant. the probability of switching over to model M_j at the next $(k+1)^{th}$ instant is p_{ij}. The mode selected using the Markov chain is assumed to be among the possible modes of the set M. The set of modes M may consist of several maneuver models.

2.2 Target Motion Models

The most common forms of target motion models are: 1)2nd order kinematic model (constant velocity model), 2) 3rd order kinematic model (constant acceleration .model)

2.2.1 Constant VelocityModel

The 2nd order kinematic model. with position and velocity components in each of the two Cartesian coordinates x and y, has the following transition and process noise gain matrices.

$$F = \begin{bmatrix} 1 & T & 0 & 0 & 0 & 0 \\ 0 & 1 & 0 & 0 & 0 & 0 \\ 0 & 0 & 0 & 0 & 0 & 0 \\ 0 & 0 & 0 & 1 & T & 0 \\ 0 & 0 & 0 & 0 & 1 & 0 \\ 0 & 0 & 0 & 0 & 0 & 0 \end{bmatrix} \qquad G = \begin{bmatrix} T^2/2 & 0 \\ T & 0 \\ 0 & 0 \\ 0 & T^2/2 \\ 0 & T \\ 0 & 0 \end{bmatrix} \tag{3}$$

Note that the acceleration component in the above model, though identically equal to zero, has been retained for compatibility with the 3rd order model to be discussed nest. In Eq. (3). the variations in velocity are modeled as zero-mean white noise accelerations. Low noise variance Q_1 is used with the model to represent the constant course and speed of the target in a non-maneuvering mode. The process noise intensity in each coordinate is generally assumed to be equal

$$Q_1 = \sigma_x^2 = \sigma_y^2 \tag{4}$$

Although the 2nd order model is primarily used to track the non-maneuvering mode of a target, use of higher level of process noise variance will allow the model to track maneuvering targets as well, albeit to a limited extent.

2.22 Constant Acceleration Model

The 3rd order model with position, velocity and acceleration components in each of the two Cartesian coordinates x and y has the following transition and process noise gain matrices.

$$F = \begin{bmatrix} 1 & T & T^2/2 & 0 & 0 & 0 \\ 0 & 1 & T & 0 & 0 & 0 \\ 0 & 0 & 1 & 0 & 0 & 0 \\ 0 & 0 & 0 & 1 & T & T^2/2 \\ 0 & 0 & 0 & 0 & 1 & T \\ 0 & 0 & 0 & 0 & 0 & 1 \end{bmatrix} \qquad G = \begin{bmatrix} T^2/2 & 0 \\ T & 0 \\ 1 & 0 \\ 0 & T^2/2 \\ 0 & T \\ 0 & 1 \end{bmatrix} \tag{5}$$

The acceleration increments over a sampling period are a discrete time zero-mean white noise. A low value of process noise variance Q_2 (but relatively higher than Q_1) will yield nearly a constant acceleration motion. The noise variances in each coordinate are assumed to be equal

$$Q_2 = \sigma_x^2 = \sigma_y^2 \tag{6}$$

Studies have shown that use of higher process noise levels combined with 3rd order kinematic model can help track the onset and termination of a maneuver to a certain extent.

In addition to above mentioned kinematic models, nonlinear models derived for a target executing coordinated turn (moving at a constant speed and turning at a constant angular rate) are also used. The angular rate in these models is estimated as part of the state vector.

2.3 Steps of IMM algorithm

Figure 1 shows one cycle of a 2-model IMM estimation algorithm. Estimation with more than 2 filters poses no problem and can be performed with equal ease. However, one needs to ascertain if the improvement in the performance of algorithm is worth the expense incurred from high computational requirements. The basic IMM algorithm has four major steps:

1. *Interaction* : Using the mixing probabilities $\mu_{i|j}(k-1|k-1)$ as weighting factors, the estimates of $\hat{X}(k-1|k-1)$ and $\hat{P}(k-1|k-1)$ from the previous cycle are used to obtain the initial conditions $\hat{X}_{0j}(k-1|k-1)$ and $\hat{P}_{0j}(k-1|k-1)$ for the mode-matched filters M_1 and M_2 of the current cycle (see Fig. 1). For all $i, j \in M$, the initial conditions for the filters are given by

$$\hat{X}_{0j}(k-1|k-1) = \sum_{i=1}^{r} \hat{X}_i(k-1|k-1)\mu_{i|j}(k-1|k-1) \tag{7}$$

$$P_{0j}(k-1|k-1) = \sum_{i=1}^{r} \left[\begin{array}{l} P_i(k-1|k-1) + \\ \{\hat{X}_i(k-1|k-1) - \hat{X}_{0i}(k-1|k-1)\} \times \\ \{\hat{X}_i(k-1|k-1) - \hat{X}_{0j}(k-1|k-1)\}^T \end{array} \right] \mu_{i|j}(k-1|k-1) \tag{8}$$

where the time index is given by k ; niode-matched filters $j = 1, \ldots, r$; models $i = 1, \ldots r$ $r = 2$ for the 2-model IMM approach; $\hat{X}_i(k|k)$ and $P_i(k|k)$ are the state estimate and

covariance in mode i; and $\hat{x}_{0j}(k|k)$ and $P_{0j}(k|k)$ are the mixed initial conditions for filter j at time k

2. *Probability Evaluations*: The mixing probabilities to be used in **Eqs.** (7) and **(8)** are computed as follows:

$$\mu_{ij}(k-1|k-1) = \frac{1}{\bar{c}_j} p_{ij}\mu_i(k-1) \tag{9}$$

where $$\bar{c}_j = \sum_{i=1}^{r} p_{ij}\mu_i(k-1) \tag{10}$$

$\mu_i(k)$ is the mode probability at time k and $\bar{c}_j$ is a normalization factor. p_{ij} is the Markov transition probability which takes care of the switch from mode i to mode j. This is a design parameter and is chosen by the user. The switching probabilities are generally known to depend upon *sojourn* time. For example, consider the following Markov chain transition matrix between the two modes of the IMM

$$p_{ij} = \begin{bmatrix} 0.9 & 0.1 \\ 0.33 & 0.67 \end{bmatrix}$$

The basis for selecting $p_{12} = 0.1$ is that, in the initial stages, the target is likely to be in non-maneuvering mode and probability to switch over to maneuvering mode will be relatively low. On the other hand, p_{22} is selected based on the number of sampling periods for which the target is expected to maneuver (*sojourn* time). If the target maneuver lasts for 3 sample periods ($\tau = 3$), the probability p_{22} is given by

$$p_{22} = 1 - \frac{1}{\tau} = 0.67 \tag{11}$$

To compute $\mu_{ij}(k|k)$ and $\bar{c}_j$ in **Eqs. (9)** and (10) in the first cycle of estimation algorithm, the initial mode probabilities $\mu_i(k)$ corresponding to non-maneuver and maneuver mode can be taken as 0.9 and 0.1, respectively. This selection is based on the assumption that the target is more likely to be in nap-maneuver mode than in maneuver mode during the initial stages of target motion. For subsequent computations, the mode probabilities are updated using the following relation

$$\mu_j(k) = \frac{1}{c}\Lambda_j(k)\bar{c}_j \qquad j = 1,\ldots,r \tag{12}$$

where $\Lambda_j(k)$ represents the likelihood function corresponding to filter j (see **Eq.** (17)) and the normalizing factor c is given by

$$c = \sum_{j=1}^{r} \Lambda_j(k)\bar{c}_j \tag{13}$$

3. *Mode-conditioned filtering*: With r parallel mode-matched Kalman Filters ($r = 2$ for 2-model IMM). the states and covariances are estimated using the standard prediction and update steps.

$$\hat{X}_j(k|k-1) = F_j(k-1)\hat{X}_{0j}(k-1|k-1) + G_j(k-1)w_j(k-1)$$

$$P_j(k|k-1) = F_j(k-1)P_{0j}(k-1|k-1)F_j(k-1)^T + G_j(k-1)Q_j(k-1)G_j(k-1)^T \quad (14)$$

$$\hat{X}_j(k|k) = \hat{X}_j(k|k-1) + K_j(k)v_j(k)$$

$$P_j(k|k) = P_j(k|k-1) - K_j(k)S_j(k)K_j(k)^T$$

If the measurements through time k are given by $Z(k)$, the measurement prediction $\hat{Z}_j(k|k-1)$ is given by the relation

$$\hat{Z}_j(k|k-1) = H_j(k)\hat{X}_j(k|k-1) \quad . \quad (15)$$

The residual $v_j(k)$, residual covariance $S_j(k)$ and the filter gain $K_j(k)$ in Eq. (14) are given by

$$v_j(k) = Z(k) - \hat{Z}_j(k|k-1)$$

$$S_j(k) = H_j(k)P_j(k|k-1)H_j(k)^T + R_j(k) \quad (16)$$

$$K_j(k) = P_j(k|k-1)H_j(k)^T S_j(k)^{-1}$$

Note that the structure of the system given by F and H matrices, and the process and measurement noise covariance matrices given by Q and R, can differ from mode to mode. The likelihood function for mode-matched filter j is a Gaussian density function of residual v with zero mean and covariance S. It is computed as follows

$$\Lambda_j(k) = \frac{1}{\sqrt{|S_j(k)|\,(2\pi)^{n/2}}} e^{-0.5[v_j(k)^T S_j(k)^{-1} v_j(k)]} \quad (17)$$

where n denotes the dimension of the measurement vector Z ($n=2$ in the present case).

4. *Overall state and covariance estimate* : The average mode probabilities obtained in Eq.(12) are used as weighting factors to combine the updated state and covariance from Eq. (14), for all filters ($j = 1,...,r$), to obtain overall state estimate and covariance.

$$\hat{X}(k|k) = \sum_{j=1}^{r} \hat{X}_j(k|k)\mu_j(k)$$

$$P(k|k) = \sum_{j=1}^{r} \left\{ P_j(k|k) + [\hat{X}_j(k|k) - \hat{X}(k|k)][\hat{X}_j(k|k) - \hat{X}(k|k)]^T \right\} \mu_j(k) \quad (18)$$

2.4 Design Parameteis of IMM

The IMM design parameters are : 1) the model set M consisting of possible target modes, e.g., constant velocity model, constant acceleration and coordinated turn models. 2) process noise variances for the adopted models. Target motion can be tracked using a low-level process noise covariance matrix with non-maneuvering model and a high-level process noise with maneuvering model. 3) the mode transition probabilities to switch from one model to another

An example target trajectory. taken from a monograph on target tracking, forms the 1st Data set for the current investigations [Ref. 2]. The data is generated using a third order kinematic model with process noise acceleration increments (see Eq. (5)) and additional arbitrary accelerations. With a sampling interval of I sec, a total of 20 scans ($k = 20$) are generated. The data simulation proceeds with the following assumed parameter values [Ref. 2]

- initial state $(x, \dot{x}, \ddot{x}, y, \dot{y}, \ddot{y})$ of target is (0.1E+03, 0.3E+02, 0.0, 0.1E+03, 0.2E+02, 0.0)
- Process noise variance Q=0 1. It is assumed that $Q_{xx} = Q_{yy} = Q$
- Measurement noise variance R =25. It is assumed that $R_{xx} = R_{yy} = R$

It is further assumed that, the target has an additional acceleration of (x_{acc}, y_{acc}) at scan 8 and an acceleration of $(-x_{acc}, -y_{acc})$ at scan IS (see Fig. 2). Data simulation is carried out using the base state model defined in Eq. (I) with process noise vector w (which is a 2x1 matrix) modified to include additional accelerations at the specified scan points.

$$\left.\begin{aligned} w(1) &= guass() * \sqrt{Q_{xx}} + x_{acc} \\ w(2) &= guass() * \sqrt{Q_{yy}} + y_{acc} \end{aligned}\right\} \text{ at scan 8}$$

$$\left.\begin{aligned} w(1) &= guass() * \sqrt{Q_{xx}} - x_{acc} \\ w(2) &= guass() * \sqrt{Q_{yy}} - y_{acc} \end{aligned}\right\} \text{ at scan 15} \qquad (20)$$

At the other scan points (i.e., $k = 1,...,7$ and $k = 9,...14$ and $k = 16,...20$), the vector w is simply defined by

$$\begin{aligned} w(1) &= guass() * \sqrt{Q_{xx}} \\ w(2) &= guass() * \sqrt{Q_{yy}} \end{aligned} \qquad (21)$$

Acceleration magnitudes of $x_{acc} = 5m/s^2$ and $y_{acc} = -6m/s^2$ are used in Eqs. (19) and (20). The function $guass()$ uses a central-limit theorem to generate Gaussian random numbers with mean 0 and variance 1. Figure 3 shows the target x and y positions under the influence of additional acceleration.

Data Set II for a maneuvering target is simulated in MATLAB using the 2nd order (Model 1) and 3rd order (Model 2) models defined in Eqs. (3-6). With sampling interval of 1 sec, a total of 60 sec data ($k = 60$) is generated. The simulation proceeds with the following input parameters:

- initial state $(x, \dot{x}, \ddot{x}, y, \dot{y}, \ddot{y})$ of target is (1 1097.6 -6.20 3425 -299.90 40 0 0)
- A low-level process noise variance of $Q1$=0.09 is considered for Model 1 when the target is not maneuvering. On the other hand, a higher value of Q2=36 is assumed to simulate the maneuvering phase of the flight with Model 2. For both models, the

noise variances in each coordinate x and y are assumed to be equal, e.g., $Q_{xx} = Q_{yy} = Q$

- Measurement variance $R = 100$. It is assumed that $R_{xx} = R_{yy} = R$.

Figure 4 shows the use of Model 1 and Model 2 to generate the target trajectory. It is seen that at scan 10, additional accelerations $x_{acc} = -35.35, y_{acc} = +35.35$ are given in x and y directions to simulate the first turn in target trajectory and at scan 35, $x_{acc} = +24.74, y_{acc} = -24.74$ are given to simulate the second turn. In other words, with state vector defined as

$$X = [x, \dot{x}, \ddot{x}, y, \dot{y}, \ddot{y}] .$$

and the state model defined as

$$x(k+1) = F_j(k)x(k) + G_j(k)w_j(k)$$
$$z(k) = H_j(k)x(k) + v_j(k)$$

data simulation is carried out with

$\ddot{x} = 0, \ddot{y} = 0$	at scan 1 (initial state)
$\ddot{x} = -35.35 m/s^2, \ddot{y} = +35.35 m/s^2$	at scan 10
$\ddot{x} = -24.74 m/s^2, \ddot{y} = +24.74 m/s^2$	at scan 35

4 Results and Discussion

The estimation algorithms are evaluated based on their tracking performance, accuracy and consistency Estimated mode probabilities from IMM are plotted to verify maneuver detection abilities of the approach Results showing sensitivity of IMM to design parameters are also presented and discussed.

Figures 5 and 6 illustrate the tracking performance of IMM and KF with Data Set I and II, respectively. While KF uses a single constant velocity model with high-level process noise variance. IMM uses 2 rnode-matched filters with low and high-level process noise variances to track the target through different modes. For analysis with IMM, the transition probability matrix selected for Data set I and I1 is, respectively

$$p_{ij} = \begin{bmatrix} 0.9 & 0.1 \\ 0.0667 & 0.9333 \end{bmatrix} \quad \text{and} \quad p_{ij} = \begin{bmatrix} 0.9 & 0.1 \\ 0.1429 & 0.8571 \end{bmatrix}$$

The above choice is made keeping in view the sojourn time ($\tau = 7$ for Data Set I and $\tau = 15$ for Data Set II) of the target. Eq. (11) is used to arrive at the p_{22} value in the above transition matrices. The comparison of estimated trajectories from IMM and KF with measured trajectory is reasonably good. Some discrepancies are observed in the maneuvering phase of the flight where IMM exhibits better performance than KF (see Fig. 6 for the enlarged view of the 2nd. turn of target flight). Figures 7 and 8 show the standard deviations (σ_{pos}) and the root sum square (RSS) errors in position obtained from applying IMM and KF to Data Set I & II. The process and measurement noise levels used in the state estimation are specified in the plots. The parameters σ_{pos} and RSS are computed using the following relations:

$$\sigma_{pos} = \sqrt{P_x + P_y}$$

where P_x and P_y are the diagonal elements P corresponding to positions x and y

$$\text{RSS} = \sqrt{(x_m - \hat{x})^2 + (y_m - \hat{y})^2}$$

where x_m, y_m are the measured and $\hat{x}, \hat{y}$ are the IMM or KF estimated position values,

In Figs 7(a) and 8(a), it is observed that the standard deviations computed from IMM are lower than that from KF when the target is not maneuvering and higher when the target is in maneuver phase. In Fig. 7(b), the RSS errors from IMM and KF for Data set I are found to be comparable. However, for Data Set II in Fig. 8(b), the RSS errors from KF are found to be large compared to those from IMM, indicating that despite high-level process noise variance, KF is unable to satisfactorily track the target during the maneuver phase. Interestingly, the standard deviation plot for IMM at the end of "Turn 1" in Fig. 8(a) develops an unexpected peak. Such overshoots in estimation errors *can* happen when there is a sudden onset or termination of a maneuver. IMM is generally able to correct these peaks within one or two sampling periods.

In Figs. *5* and *6* discussed earlier, the estimated trajectory was shown to have discernible differences from the measured trajectory, particularly in the maneuver phase. This degradation in tracking the target during maneuver is truthfully reflected in IMM by way of large standard deviation and RSS errors (see Figs. 7(a) and 7(b)). Although KF shows a similar increase in RSS error in Fig: 7(b), a corresponding increase in standard deviation from KF during the maneuvering phase is not visible in Fig. 7(a). This limitation of KF to compute correct values of standard deviations can lead to erroneous fusing of data fiom multiple sensors for processes that are based on covariance of the state estimates. It should also be noted that the RSS errors fiom IMM in Fig. 8(b) appear small and are not commensurate with the increased standard deviation during the same period in Fig. 8(a). Thus, IMM too can be inconsistent and may, at times, have RSS errors that are "optimistic". Nonetheless. the calculated standard deviations. which (almost always) reflect the true picture of the IMM estimator performance. can still be used for data fusion purposes.

4.1 Estimated Mode probability

Figures 9 and 10 show the average mode probabilities computed from IMM for Data set I and II. In Fig. 9, the non-maneuvering mode has about 90% probability until the onset of maneuver at scan $k = 8$. Thereafter, the probability of non-maneuver mode declines and that of maneuver mode rises sharply. This indicates rapid detection of maneuver by IMM. At the termination of maneuver at scan $k = 15$, the non-maneuver mode probability starts increasing once again and the maneuver mode probability decays. Similar observations are made for Data set II in Fig. 10.

4.2 Sensitivity to Design Parameters

The design parameters of IMM consist of 1) the model set comprising of various modes. 2) the process noise intensities to cover different target regimes, and 3) and the transition probabilities to switch from one mode to another. The process noise levels are selected based on the espected magnitude of maneuvers. For example, KF uses permanently a large process noise variance to track a maneuvering target. The transition probabilities can be selected based

on the espected *sojourn* time in various modes. Choice of an appropriate measurement noise covariance matrix can also help to improve the estimator performance to a certain extent.

4.2.1 Sensitivity to process noise variance

The RSS position errors in Data Set I and II, computed using IMM and KF with different process noise levels. are shown in Figs. 11 and 12. respectively. It is observed that an incorrect choice of process noise level can degrade the performance of the estimator in the maneuver phase. In case of IMM, a lower process noise Q_1 for non-maneuver mode and a higher process noise Q_2 for maneuver mode seem to be the best choice. Although high values for both Q_1 and Q_2 also yield satisfactory results, a low process noise level when the target is not maneuvering is generally preferred. As expected, KF performs well only with a large process noise variance (see Figs. 11(b) and 12(b)).

4.2.2 Sensitivity to measurement noise variance

The RSS errors in position computed with different measurement noise levels in IMM and KF for Data set. I and II are shown in Figs. 13 and 14. Other design parameters remaining same, a smaller value for the measurement noise covariance matrix is seen to yield better accuracy in the maneuvering phase of the target motion.

4.2.3 Sensitivity to mode transition probability

As already explained earlier in the test, the rationale of choosing the maneuver onset probability p_{12} is that the maneuver is likely to start with a relatively low probability. The choice of p_{22} on the other hand is related to the expected *sojourn* time τ through Eq. (11). Figures 15 and 16 show the effect of maneuver onset probability p_{12} on maneuver detection and estimator accuracy. As seen in Fig. 15(a), there is a delay on part of the algorithm to realise the onset of maneuver when the value of $p_{12} = 0.02$. On the other hand, the estimator is quick in adapting to the changing target mode when $p_{12} = 0.1$. Any further increase in values of p_{12}, however, did not hasten the change from non-maneuver to maneuver mode (plots not shown). The RSS errors in Figs. 15(b) and 16(b) are found to be lower with $p_{12} = 0.1$. Figures 17(a) and 17(b) show the effect of *sojourn* time τ on RSS errors computed from IMM for Data set I and II. The *sojourn* time for Data set I is 8 secs (period for which the target is in maneuver phase) and that for Data set II is 15 secs (for each Turn 1 and Turn 2 of target flight). In real flight scenario, the actual *sojourn* time will not be exactly known and only anticipated values of τ will have to be used in Eq. (11) to compute p_{22}. It is concluded from Fig. 17 that higher values of τ ($p_{22} \cong 0.95$) should be selected for better accuracy in estimation.

5 Concluding Remarks

IMM and KF tracking algorithms are implemented in MATLAB and applied to simulated data of a target whose flight path changes with time. Sensitivity of IMM to process and measurement noise levels, and to mode transition probabilities is investigated. The IMM exhibits an overall better performance and is very suitable for tracking maneuvering targets.

[1] Yakkov Bar-Shalom and Xiao-Rong Li, "Multitarget-Multisensor Tracking : Principles and Techniques", 1995 (ISBN 0-9648312-0-1).

[2] Yakkov Bar-Shalom, "Multimodel Data Association Tracker", 1991 (ISSN 0895-9129).

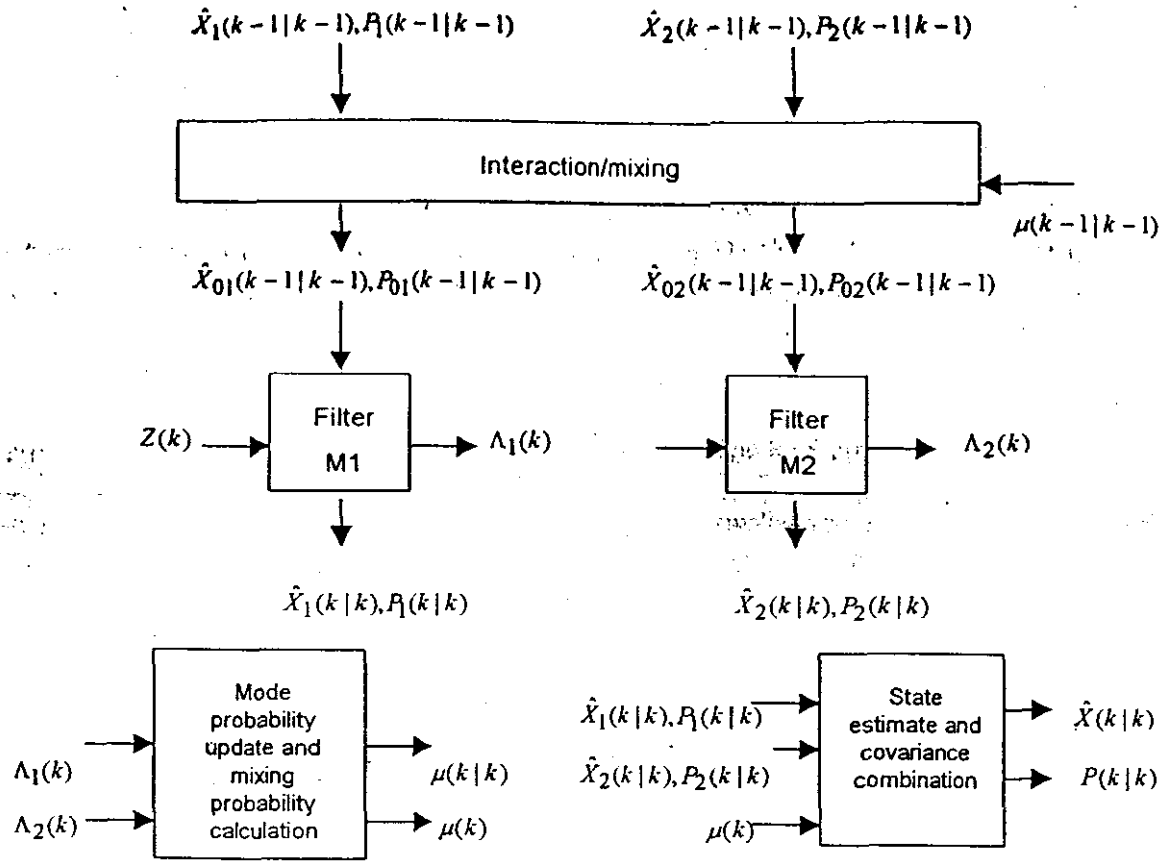

Fig. 1 A schematic showing one cycle of 2-model IMM estimation algorithm

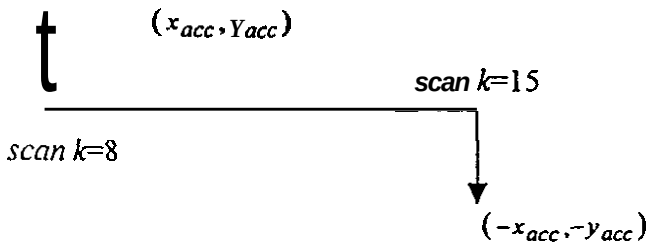

Fig. 2 Target Acceleration Model for simulation of Data Set I

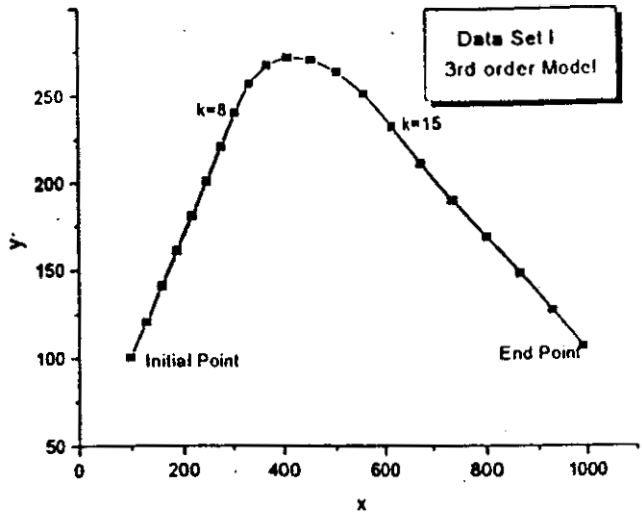

Fig. 3 Simulation of Data Set I with 3rd order kinematic model

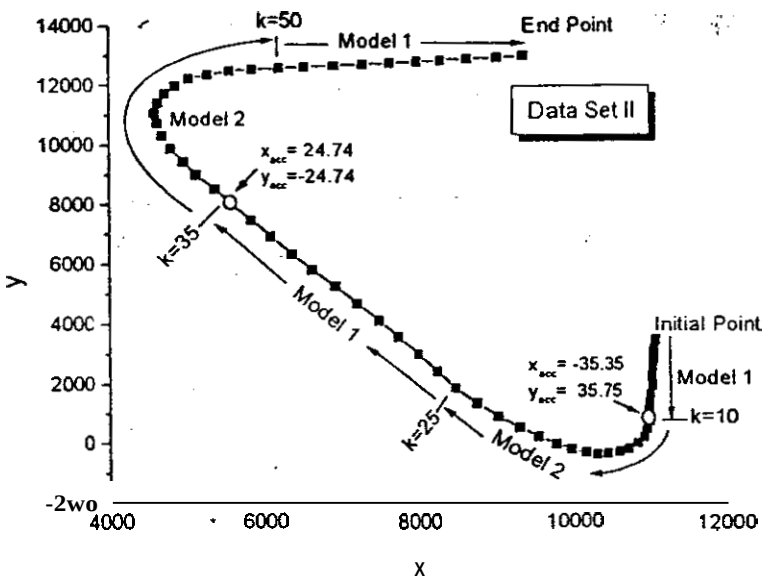

Fig. 4 Simulation of Data Set II with 2nd and 3rd order kinematic models

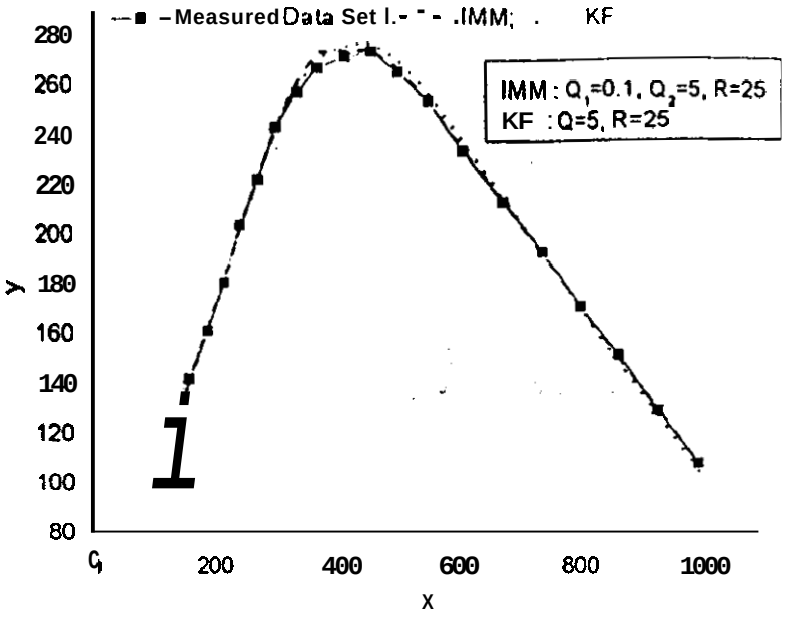

Fig. 5 Tracking performance of IMM and KF with Data Set I

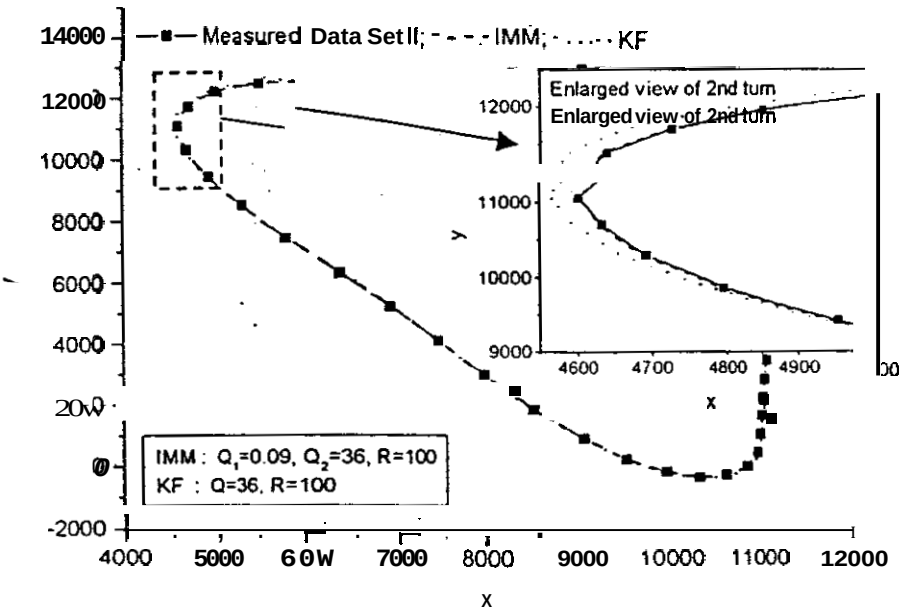

Fig. 6 Tracking performance of IMM and KF with Data Set II

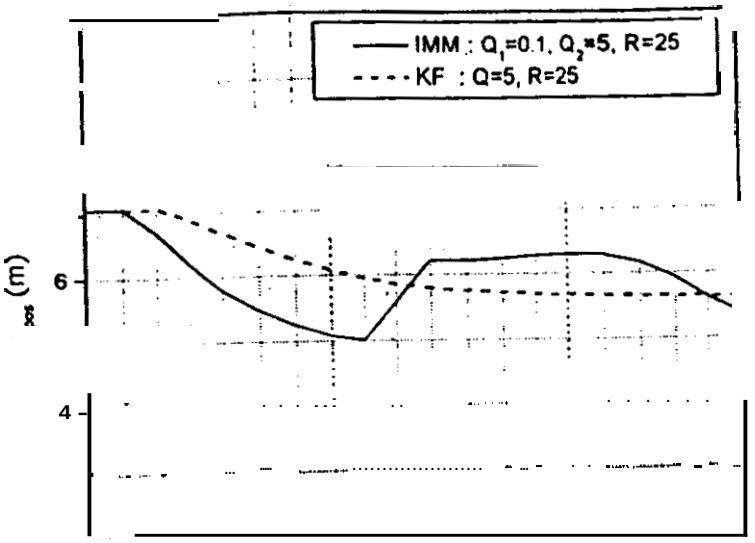

Fig. 7(a) Estimated Standard Deviations from Data Set I

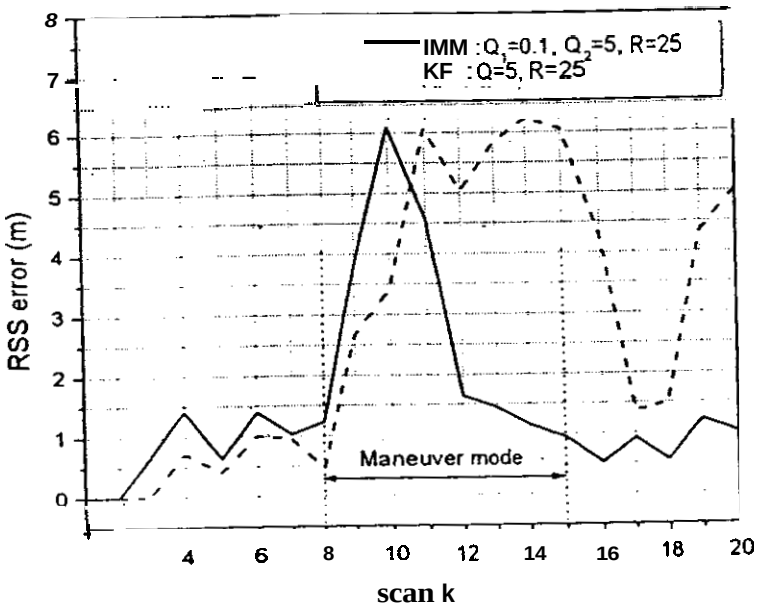

Fig. 7(b) Root Sum Square errors in position from Data Set I

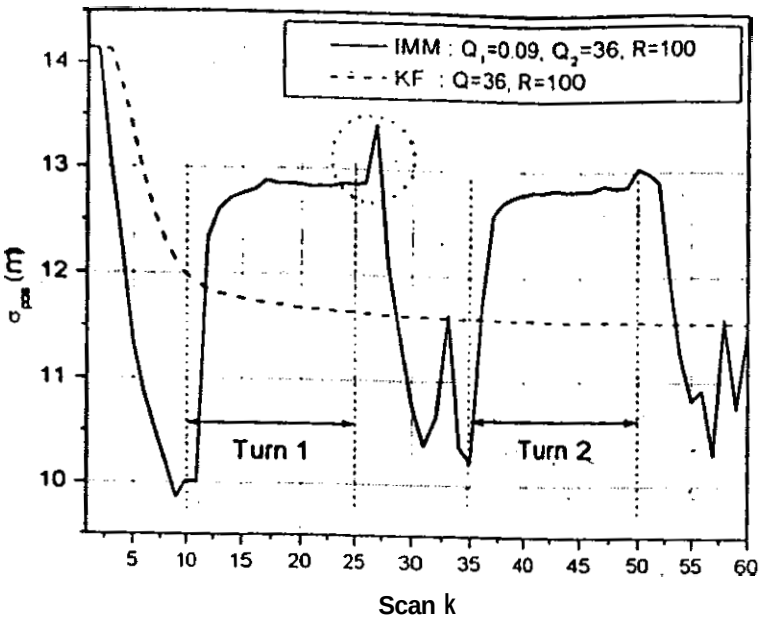

Fig. 8(a) Estimated Standard Deviations from Data Set II

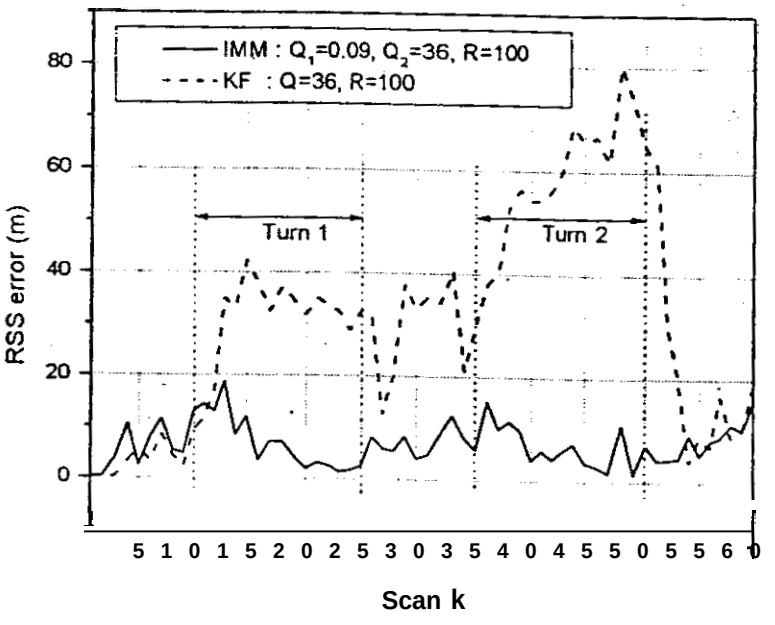

Fig. 8(b) Root Sum Square errors in position from Data Set II

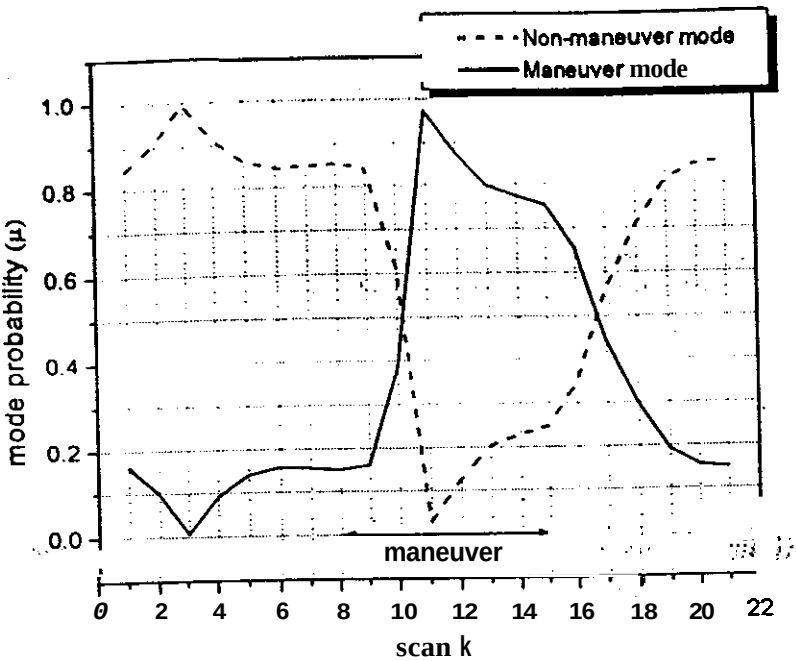

Fig. 9 Estimated mode probabilities for Data Set I using IMM

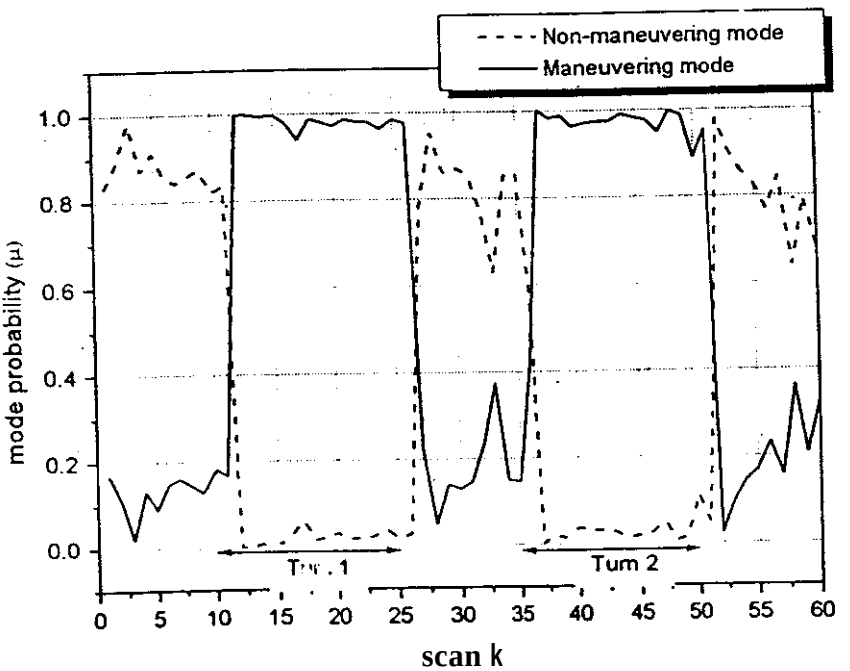

Fig. 10 Estimated mode probabilities for Data Set II using IMM

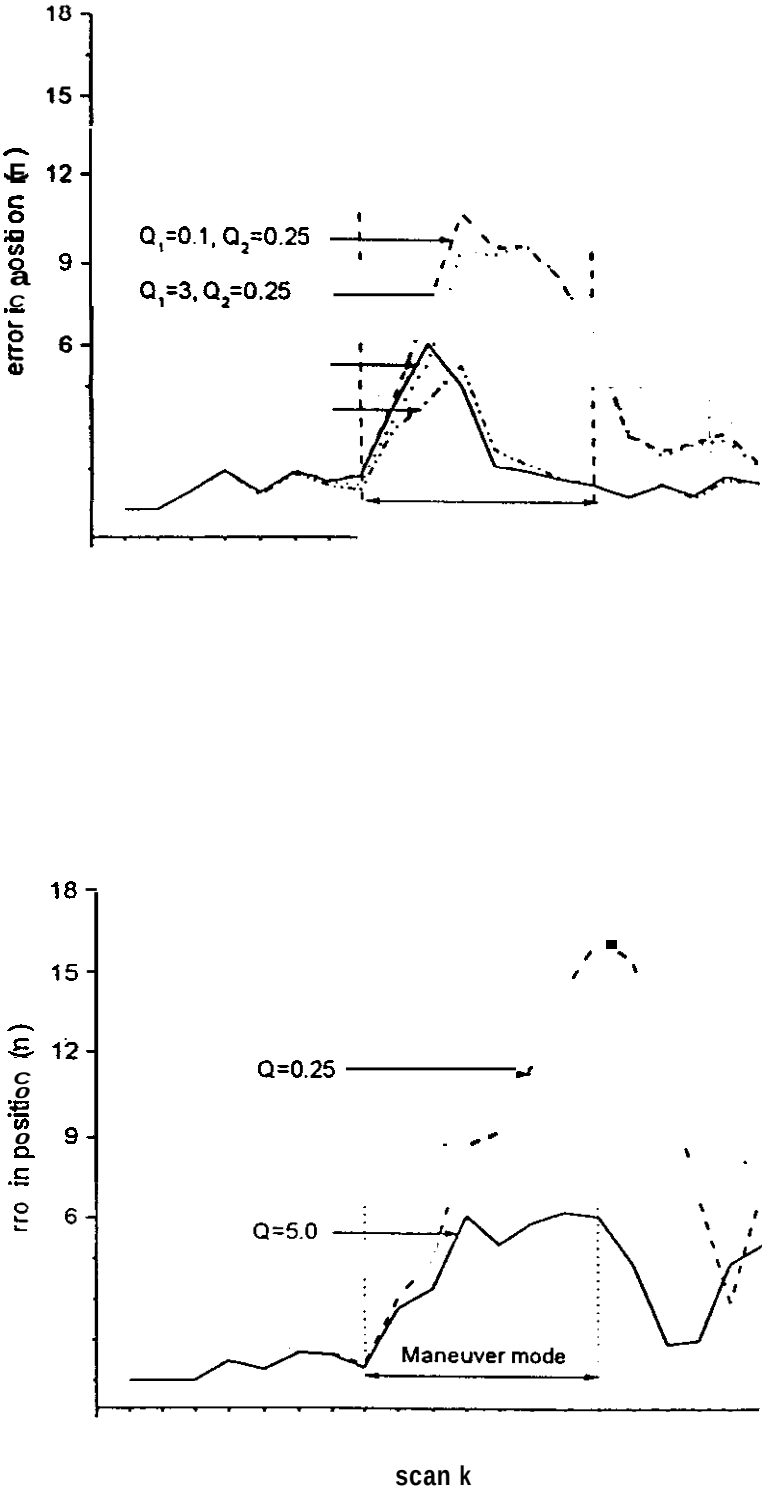

Fig. 11(b) Root sum square errors in position obtained from analysis of Data Set I with KF for low and high process noise intensities

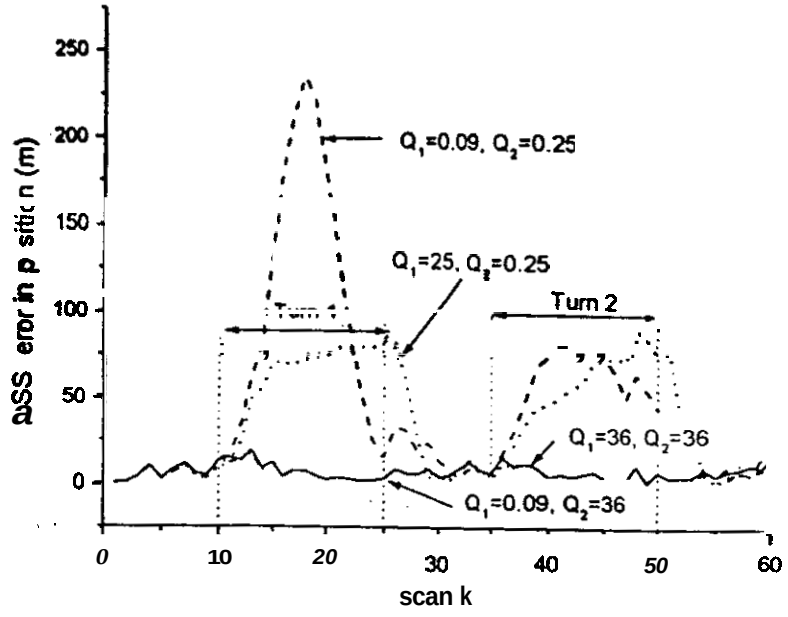

Fig. 12(a) Root sum square errors in position obtained from analysis of Data Set II with IMM for different process noise intensities

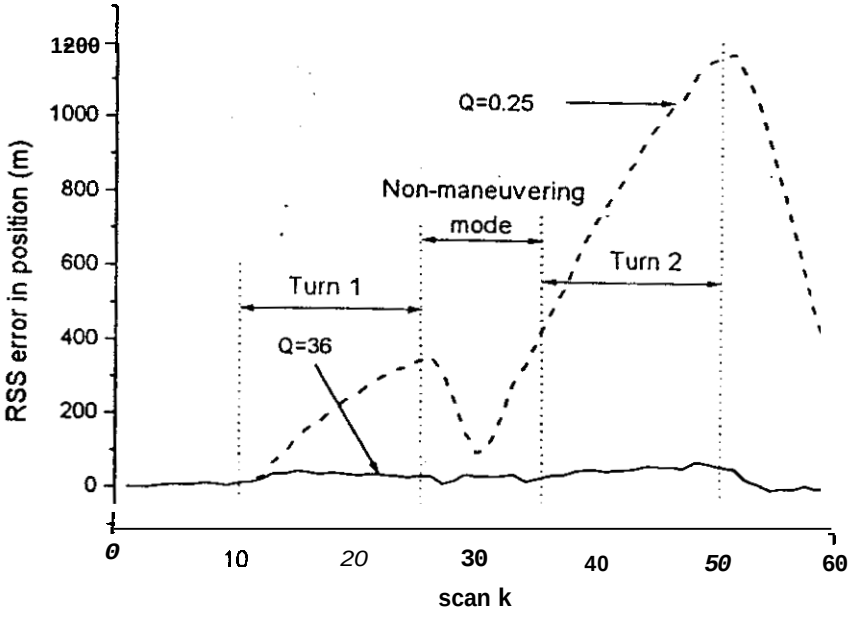

Fig. 12(b) Root sum square errors in position obtained from analysis of Data Set II with KF for low and high process noise intensities

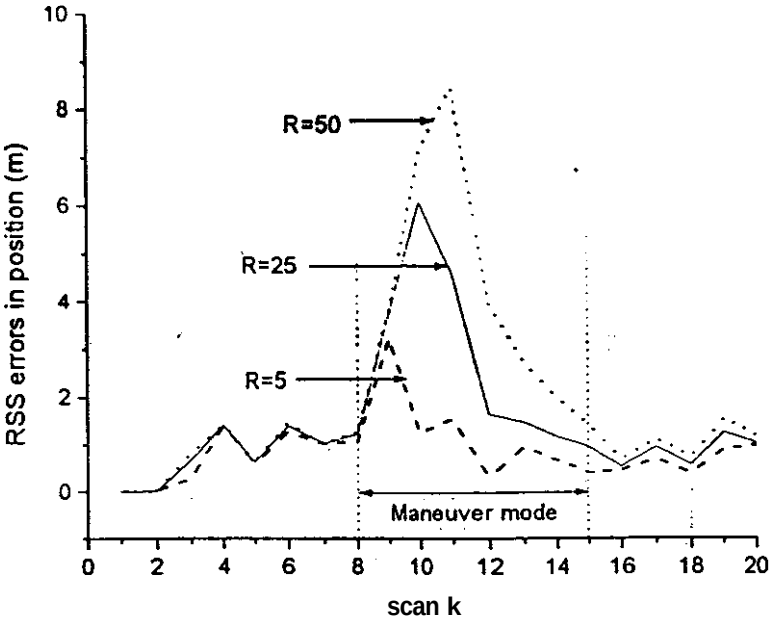

Fig. 13(a) Root sum square errors in position obtained from analysis of Data Set I with IMM for different measurement noise intensities

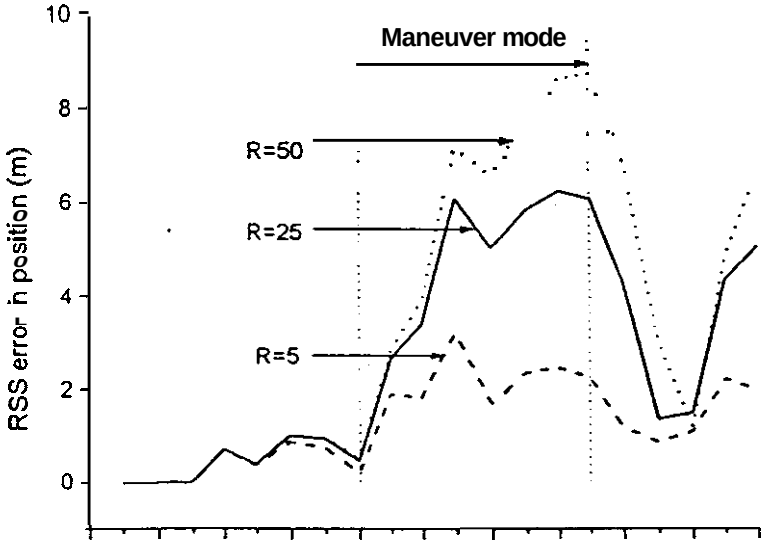

Fig. 13(b) Root sum square errors in position obtained from analysis of Data Set I with KF for different measurement noise intensities

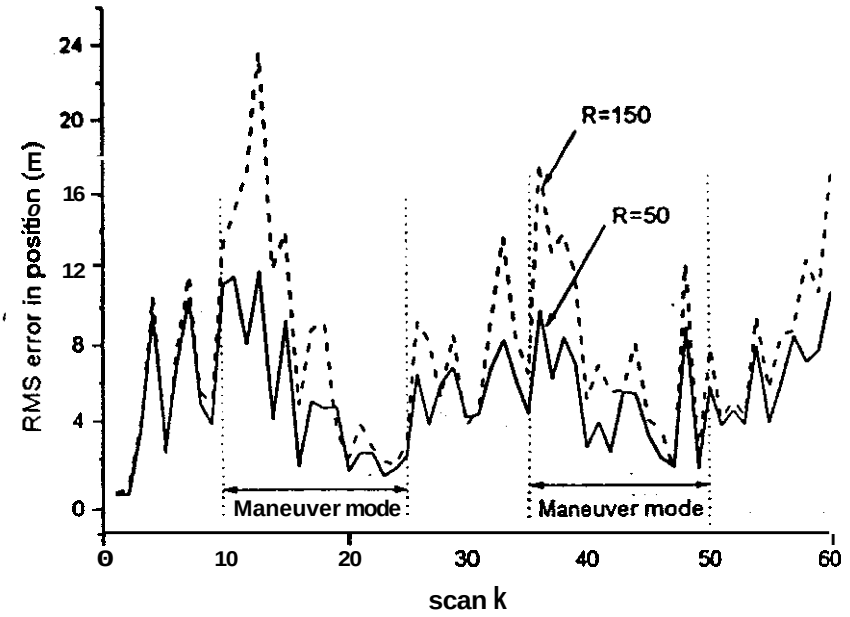

Fig. 14(a) Root sum square errors in position obtained from analysis of Data Set II with IMM for different measurement noise intensities

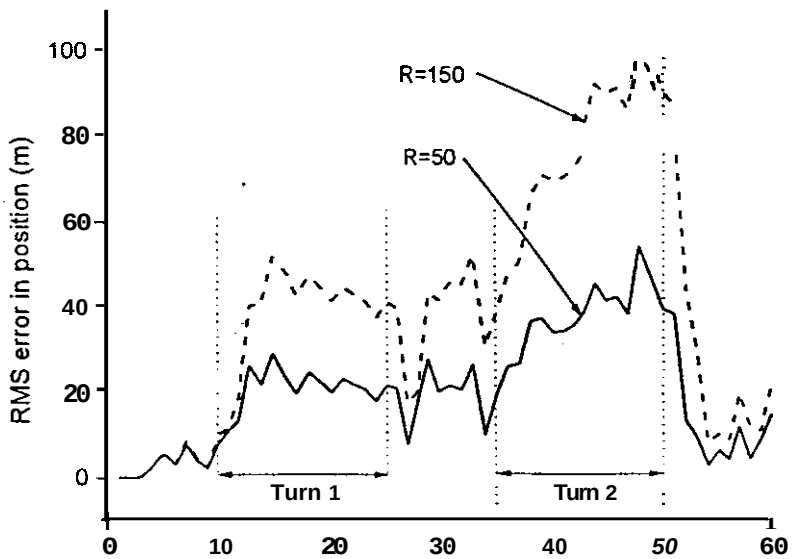

Fig. 14(b) Root sum square errors in position obtained from analysis of Data Set II with KF for different measurement noise intensities

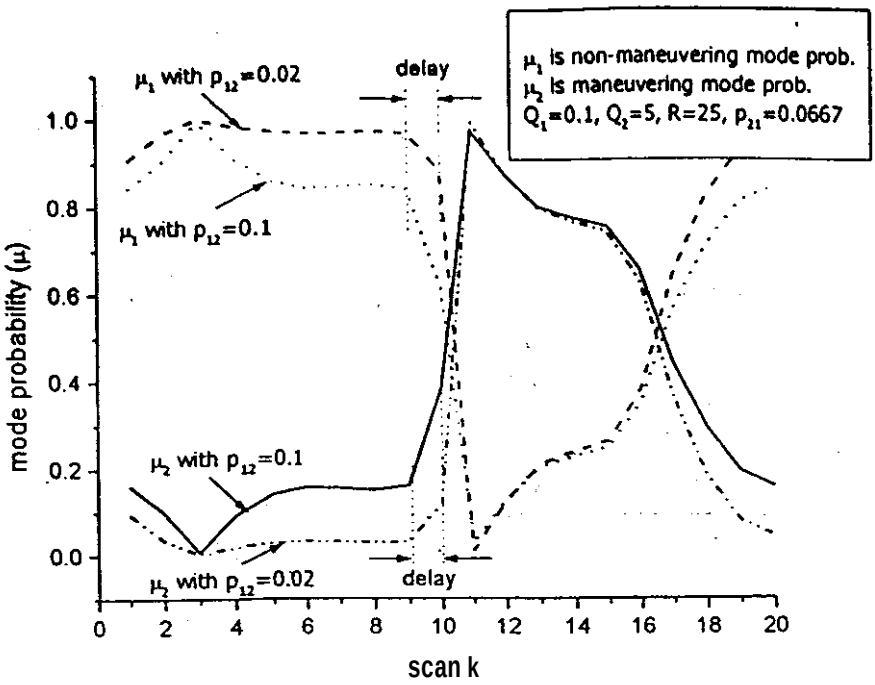

Fig. 15(a) Effect of transition probability on maneuver detection with IMM (Data Set I)

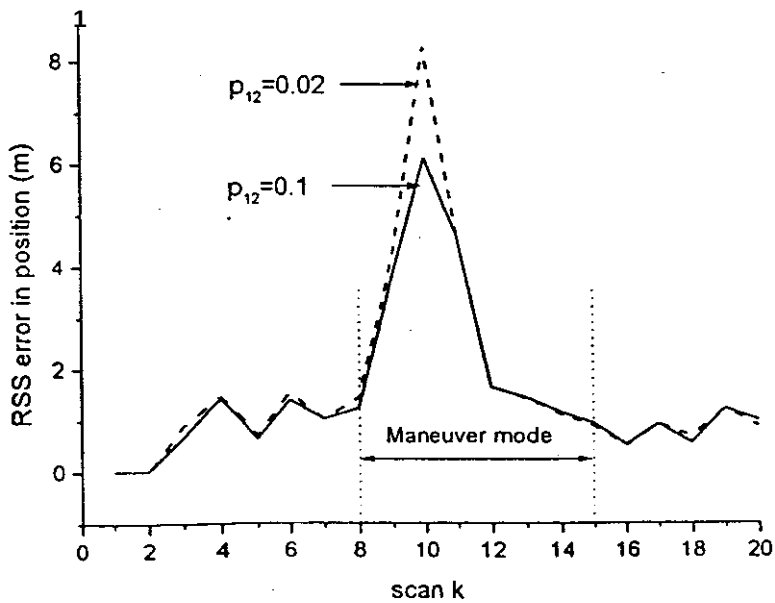

Fig. 15(b) Effect of maneuver oiiset probability p_{12} on estimator accuracy (Analysis of Data Set I with IMM)

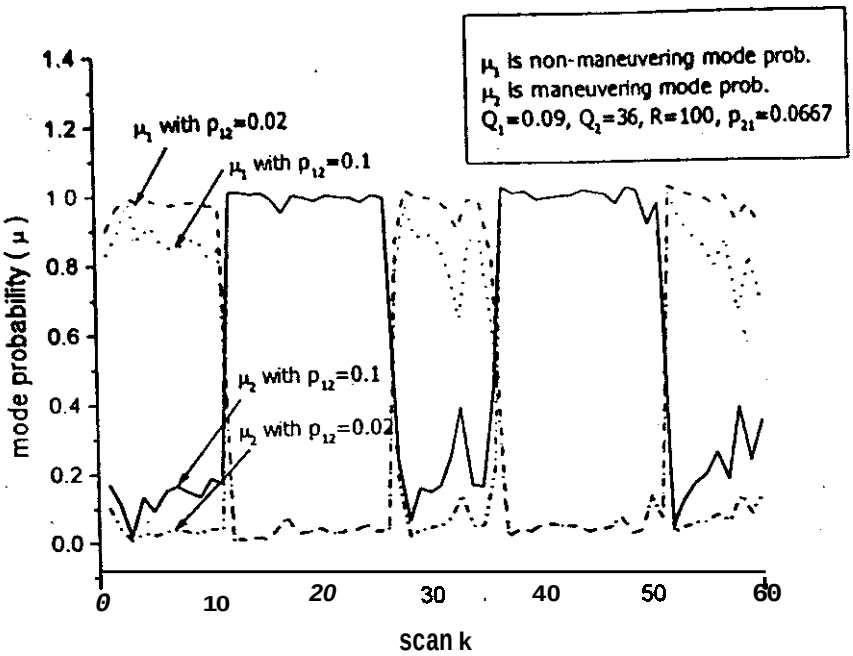

Fig. 16(a) Effect of transition probability on maneuver detection with IMM (Data Set II)

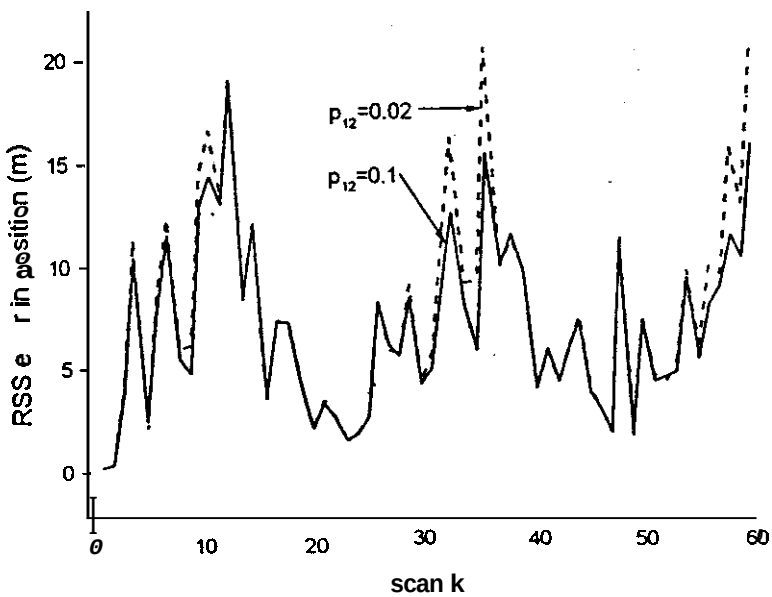

Fig. 16(b) Effect of maneuver onset probability p_{12} on estimator accuracy (Analysis of Data Set II with IMM)